Precision measurement of the Stark shift in the $6S_{1/2} \rightarrow 6P_{3/2}$ cesium transition using a frequency-stabilized laser diode

Carol E. Tanner and Carl Wieman
Joint Institute for Laboratory Astrophysics, University of Colorado and National Bureau of Standards, Boulder, Colorado 80309-0440 and Physics Department, University of Colorado, Boulder, Colorado 80309
(Received 21 December 1987)

We employ crossed-beam laser spectroscopy with a frequency-stabilized laser diode to measure the Stark shift of the $6P_{3/2}$ state relative to the ground state of atomic cesium. The scalar and tensor polarizabilities are determined from the measured Stark shifts in the transitions $6S_{1/2}\,F=4 \rightarrow 6P_{3/2}\ F'=5$, $M_F=5$ and 4. Our results are $\alpha_0(6P_{3/2})+\alpha_2(6P_{3/2})-\alpha_0(6S_{1/2})=977.8(19)a_0^3$ and $\alpha_2(6P_{3/2})=-262.4(15)a_0^3$.

The low-lying electronic states of Cs are being studied extensively in our laboratory because of their connection to the investigation of parity nonconservation (PNC) in the $6S_{1/2} \rightarrow 7S_{1/2}$ transition.[1] This paper describes the precise measurement of the Stark shift in the $6S_{1/2} \rightarrow 6P_{3/2}$ transition from which we determine the electric dipole polarizability of the $6P_{3/2}$ state. Interpretation of PNC measurements involves atomic-structure calculations that include sums of radial integrals. The Stark effect provides an important test of these calculations since it is the only precisely measurable quantity that depends on these matrix elements. The Stark effect in the Cs $6P_{3/2}$ state was first measured by Marrus *et al.* in an atomic-beam rf resonance experiment,[2] but they did not achieve the precision necessary to test adequately present theoretical methods of atomic-structure calculations.[3] Hunter *et al.* have recently improved upon these measurements by using laser spectroscopy to observe the shifts of the Doppler-broadened $6S_{1/2} \rightarrow 6P_{3/2}$ transitions in a cell.[4] We set out to make a careful study of the Stark effect in the Cs $6P_{3/2}$ state in order to improve the precision and because of a possible discrepancy between theory and experiment (now resolved) in the tensor polarizability.[5]

The Hamiltonian describing the interaction between an atom and external electric field, to lowest order, is[6]

$$H=-\tfrac{1}{2}\alpha E^2\ ,$$

$$\alpha=\alpha_0+\alpha_2 Q_{F'',F';M_F}\ , \tag{1}$$

where α is the polarizability describing the induced electric dipole moment of the atom. The polarizability of $P_{3/2}$ states contains both scalar α_0 and tensor α_2 parts. The scalar part shifts all hyperfine and magnetic sublevels $P_{3/2}\ F'\ M_F$, equally. The tensor part mixes states of different F' through the matrix Q (see Ref. 6), but M_F remains a good quantum number. This causes each magnetic sublevel $|M_F|$ to shift by a different amount.[7,8]

There are significant experimental difficulties involved in separating the scalar and tensor parts of the interaction because α_2 is small. If the M_F levels are not resolved, as in the previous measurements of the polarizability of the Cs $6P_{3/2}$ state, one must accurately fit the resonance line shape by including all M_F levels to extract α_0 and α_2 independently. This requires precise knowledge of the population of each sublevel but many things, especially optical pumping, can lead to nonthermal populations. We avoid these difficulties by resolving the M_F levels. This is achieved by performing laser spectroscopy on a Cs atomic beam with a resolution near that of the natural linewidth of the $6P_{3/2}$ state (5 MHz) in fields up to 45 kV/cm. Figure 1 is a frequency scan of the $6P_{3/2}\ F'=5$ (plus a small admixture of $F'=4$) state showing the M_F substructure at 40 kV/cm. The $|M_F|=5$, 4, and 3 levels are clearly resolved, while $|M_F|=0$, 1, and 2 still overlap. The energy shifts of the resolved levels are only a function of E and are not affected by optical pumping. We use a fixed-frequency laser with part of its output shifted in frequency by an acousto-optic modulator to find the shifts in the $|M_F|=5$ and 4 transition line centers. This technique has the advantage of measuring only frequency differences, without the many uncertainties involved in precise wavelength measurements.

The apparatus is shown schematically in Fig. 2. A

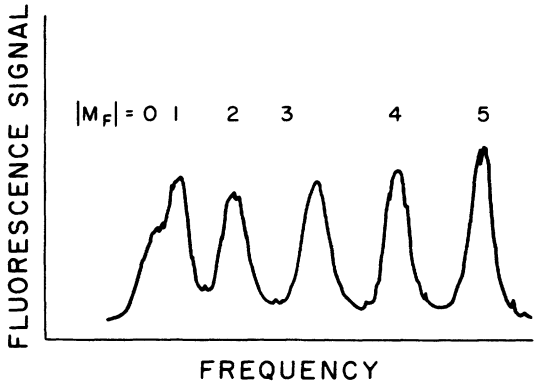

FIG. 1. Laser frequency scan showing the M_F substructure of the $6S_{1/2}\ F=4 \rightarrow 6P_{3/2}\ F'=5$ transition at an electric field of 40 kV/cm. The $|M_F|=5$ and 4 lines are 38 MHz apart and 11 MHz wide.

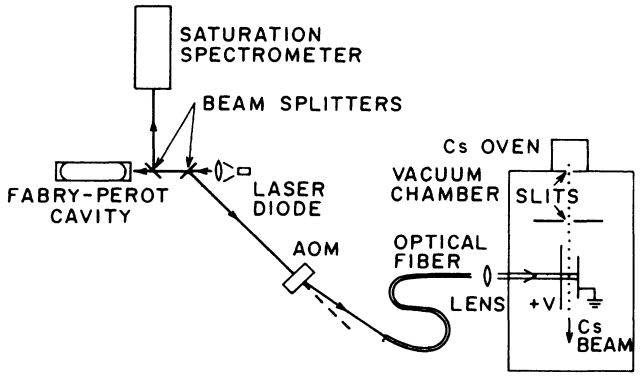

FIG. 2. Schematic of the apparatus.

beam of atomic Cs effuses from a 0.05-cm slit in an oven and is collimated with a second 0.05-cm slit 10 cm downstream. The collimated atomic beam intersects a circularly polarized laser beam at right angles in a region of high-static electric field. The laser propagation direction is aligned parallel to the static electric field. The field is produced by applying between 13 and 18 kV to a pair of coated glass plates 0.3950(2) cm apart. One plate is 5×7.5 cm^2 and has a transparent conductive coating through which the laser beam passes; the second plate is a 4.5×5.5-cm^2 gold-coated glass mirror. To assure field uniformity, the laser beam is only 0.2 cm in diameter and enters the electric field region over 2 cm (five times the plate spacing) away from the edges of the plates. As discussed in Ref. 1, the stray-field effects for these coatings are negligible. The voltage applied to the plates is measured using a high-voltage divider and a Keithley digital voltmeter. Because the divider drifts slightly with temperature, it is calibrated periodically during data collection. The fractional uncertainty in the voltage calibration is 6×10^{-4}.

The laser radiation is produced by a frequency-stabilized laser diode (Hitachi HLP1400 frequency selected for 852 nm) which is locked to a hyperfine transition in Cs. The unstabilized laser has a typical linewidth of 30 MHz and an output power of 5 mW. The frequency is stabilized by passively locking the laser to a Fabry-Perot (FP) interferometer with optical feedback from the cavity (a property unique to laser diodes). This requires only 0.8 mW of laser power and reduces the laser linewidth to much less than the 5-MHz natural width of the $6S_{1/2}\rightarrow6P_{3/2}$ transition. Although we do not have the capability to determine the laser linewidth accurately, Hollberg *et al.* have measured laser diode linewidths to be on the order of 20 kHz under similar conditions.[9]

The FP cavity gives short-term stability to the laser frequency, and long-term stability is ensured by locking the cavity to a Cs resonance line. This is accomplished by sending a portion of the laser diode beam into a Cs saturated-absorption spectrometer.[10] The saturated-absorption spectrum is produced when two counterpropagating laser beams pass through a 4-cm-long Cs vapor cell at room temperature. One beam is intense (8 mW/cm^2) and saturates the Cs transition. The second beam is a low-intensity (0.5 mW/cm^2) probe whose absorption is measured and provides Doppler-free saturation peaks superimposed on the normal Doppler-broadened absorption profile. We use another low-intensity probe to subtract off the normal Doppler-broadened profile to obtain the Doppler-free spectrum shown in Fig. 3. The FP cavity length and the laser frequency which follows it are modulated with an amplitude of 1 MHz at a frequency of 18 kHz. Phase-sensitive detection is used to obtain the first derivative of the saturated-absorption signal, and this signal is fed back to lock the cavity resonance frequency to the peak of the $6S_{1/2}\ F=4\rightarrow6P_{3/2}\ F'=5$ saturated-absorption line. Because of the narrow lines (9 MHz) and very good signal-to-noise ratio, the laser stays locked within less than 0.1 MHz of the line center. The main portion of the laser beam is shifted in frequency with one or two acousto-optic modulators (AOM). The rf driving frequency of the AOM is measured precisely with a radio-frequency counter. After the AOM, the frequency-shifted laser beam is sent through a single-mode optical fiber to ensure that the final laser beam direction remains fixed. The total laser power leaving the fiber and reaching the interaction region is about 30 μW. The fluorescence from the interaction region is detected with a cooled silicon photodiode, and the derivative of the 11-MHz wide fluorescence peak is obtained by phase-sensitive detection at the 18-kHz dither frequency.

To determine α_0 and α_2 independently, we measured two experimental parameters. One was the Stark shift of the $6S_{1/2}\ F=4\rightarrow6P_{3/2}\ F'=5\ |M_F|=5$ transition as a function of electric field, and the second was the splitting between the $|M_F|=5$ to $|M_F|=4$ sublevels of the $F'=5$ state measured at fixed voltages. The first was measured by shifting the laser frequency by known amounts between 140 and 250 MHz with the AOM. At each value of frequency shift, the voltage applied to the plates was adjusted to shift the transition into resonance.

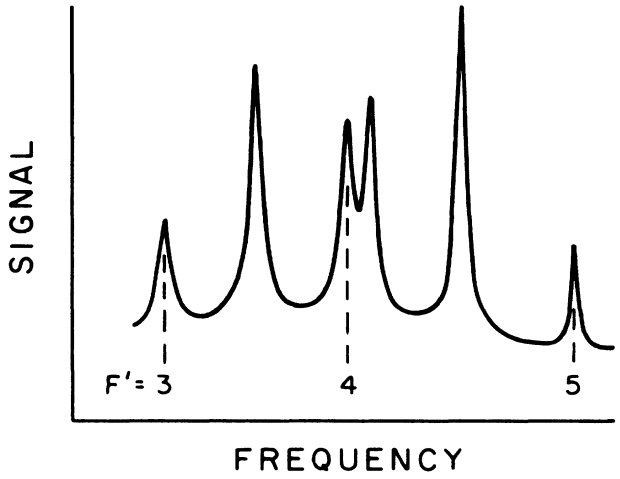

FIG. 3. Saturated absorption spectrum of the $6S_{1/2}$ $F=4\rightarrow6P_{3/2}$ F' transitions. The 9-MHz wide $F'=5$ line is used to stabilize the laser frequency. This spectrum, obtained from a single 100-ms oscilloscope sweep, shows the very large signal-to-noise ratio.

The transition line center was found by observing the zero crossing of the derivative signal. The second parameter, the $|M_F|=5$ to 4 splitting, was measured by fixing the voltage and then adjusting the AOM driving frequency to tune the frequency-shifted laser beam from one transition to the other. This measurement was repeated several times for each of three different voltage settings.

Before data were collected, we limited some possible systematic effects. First, the Cs beam was aligned perpendicular to the laser beam by adjusting the Cs beam direction while observing the zero crossing of the derivative signal at zero voltage. This reduced the Doppler shifts to less than 0.1 MHz and provided the "measurement" of zero shift at zero field. We also checked that there was no change in the measured shifts when the intensity was varied over a factor of 4. This limited possible optical-pumping effects and ac Stark shifts to less than 0.1 MHz.

The total Stark shift of the $6S_{1/2}$ $F=4\rightarrow 6P_{3/2}$ $F'=5$ $|M_F|=5$ transition as a function of electric field is

$$h\nu_5=-\tfrac{1}{2}[\alpha_0(6P_{3/2})+\alpha_2(6P_{3/2})-\alpha_0(6S_{1/2})]E^2 , \quad (2)$$

where the Stark shift in the $6S_{1/2}$ state[11] must be subtracted from the shift in the excited state. Figure 4 is a plot of this frequency shift as a function of the square of the applied voltage. Although the $|M_F|=5$ and 4 sublevels were well resolved (Fig. 1), the nearby lines pull the line centers slightly. A correction of order $+0.10(5)\%$ has been applied to account for this, but it had a negligible effect on the slope (0.01%). The frequency splitting between $6P_{3/2}$ $F'=5$ $|M_F|=5$ and $|M_F|=4$ sublevels $\nu_{54}=\nu_5-\nu_4$ was measured at three different voltage settings (also plotted in Fig. 4). For these measurements, a correction of order $+0.5(2)\%$ was added to the splittings to compensate for the pulling of the nearby lines.

The data for ν_5 fit a straight line to within the statistical uncertainties of the points, and the slope is $-0.7796(9)$ MHz/(kV)^2. We combine this slope with the plate spacing and Eq. (2) to obtain

$$[\alpha_0(6P_{3/2})+\alpha_2(6P_{3/2})-\alpha_0(6S_{1/2})]=977.8(19)a_0^3 , \quad (3)$$

where the uncertainty in this result is dominated by the uncertainty in the electric field.

Diagonalizing the Stark Hamiltonian (1) in the presence of hyperfine structure and solving for α_2 in terms of the energy splitting, one obtains

$$\alpha_2=-\frac{1}{E^2}\frac{10}{3}\frac{\left[1-\dfrac{\nu_{54}}{\nu_{\rm hf}}\right]h\nu_{54}}{\left[1-\dfrac{10}{3}\dfrac{\nu_{54}}{\nu_{\rm hf}}\right]} . \quad (4)$$

Inserting our measurements of ν_{54}, and $\nu_{\rm hf}=251.00(2)$ MHz from Ref. 12, we find

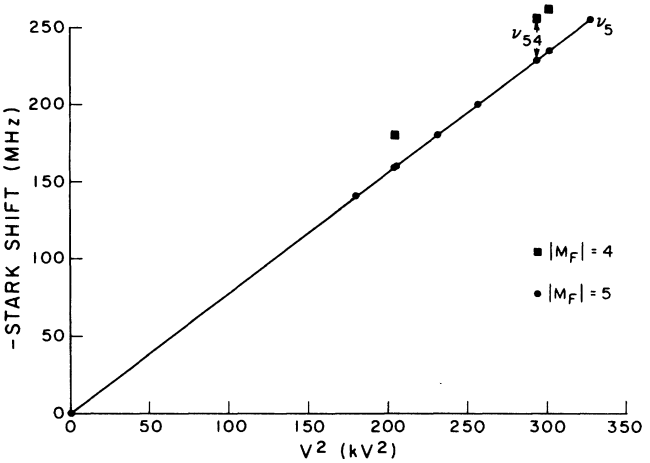

FIG. 4. Stark frequency shift as a function of voltage squared. The shift in $M_F=5$ fits a straight line. The uncertainty in each point is much less than the size of the dots on the figure.

$$\alpha_2(6P_{3/2})=-262.4(15)a_0^3 . \quad (5)$$

Combining (3) and (5) gives

$$[\alpha_0(6P_{3/2})-\alpha_0(6S_{1/2})]=1240.2(24)a_0^3 . \quad (6)$$

Our results are in good agreement with the much less precise results of Marrus. Hunter *et al.*[4] have obtained the much more recent results

$$\alpha_2(6P_{3/2})=-262(7)a_0^3 , \quad (7)$$

$$[\alpha_0(6P_{3/2})-\alpha_0(6S_{1/2})]=1264(13)a_0^3 . \quad (8)$$

Their uncertainty is larger than ours because of the broader linewidths of the transitions measured. Their value for α_2 is in good agreement with our results, but the value in (8) is different from our value (6) by slightly greater than their uncertainty.

The primary significance of our work is as a test of atomic-structure calculations. Early calculations given in Ref. 13 are in reasonable agreement with our results. Much better agreement is obtained with the recent calculations of Zhou and Norcross.[14] Using a semiempirical model potential,[15] they obtain a polarizability that agrees with our measurements to better than 1%. It will be interesting to compare our measurements to calculations using the relativistic many-body perturbation techniques that are presently being developed for high-precision atomic-structure calculations.[3]

This work was supported by National Science Foundation Grant No. PHY86-04504. We would like to acknowledge the assistance of B. P. Masterson and L. Hollberg. We would also like to thank L. R. Hunter for communicating his results to us prior to publication.

[1]S. L. Gilbert and C. E. Wieman, Phys. Rev. A **34**, 792 (1986).
[2]R. Marrus, D. McColm, and J. Yellin, Phys. Rev. A **147**, 55 (1966).
[3]W. R. Johnson, D. S. Gou, M. Idrees, and J. Sapirstein, Phys. Rev. A **32**, 2093 (1985); **34**, 1043 (1986).
[4]L. R. Hunter, D. Krause, Jr., S. Murthy, and T. W. Sung, Phys. Rev. A **37**, 3283 (1988).
[5]L. R. Hunter, D. Krause, Jr., S. Murthy, and T. W. Sung (unpublished).
[6]R. W. Schmieder, Am. J. Phys. **40**, 297 (1972).
[7]R. W. Schmieder, A. Lurio, and W. Happer, Phys. Rev. A **3**, 1209 (1971).
[8]T. M. Miller and B. Bederson, Adv. At. Mol. Phys. **13**, 1 (1977). This is an excellent review of experimental and theoretical determinations of atomic and molecular polarizabilities.
[9]B. Dahmani, L. Hollberg, and R. Drullinger, Opt. Lett. **12**, 876 (1987).
[10]W. Demtröder, in *Laser Spectroscopy,* edited by Fritz Peter Schäfer (Springer, New York, 1981), p. 489.
[11]R. W. Molof, H. L. Schwartz, T. M. Miller, and B. Bederson, Phys. Rev. A **10**, 1131 (1974). The polarizability of the Cs $6S_{1/2}$ ground state reported in this reference is $\alpha_0(6S_{1/2})=402(8)a_0^3$.
[12]C. E. Tanner and C. Wieman, Phys. Rev. A (to be publsihed).
[13]P. M. Stone, Phys. Rev. **127**, 1151 (1962).
[14]H. L. Zhou and D. Norcross (unpublished).
[15]D. Norcross, Phys. Rev. A **7**, 606 (1973).